Gamma-Ray Excitation of the 15.1-Mev Level in C^{12}†*

E. L. GARWIN
The Enrico Fermi Institute for Nuclear Studies, The University of Chicago, Chicago, Illinois
(Received October 13, 1958)

The parameters of the 15.1-Mev level in C^{12} have been determined. The angular distribution of scattered photons has been determined to be dipole. A scatterer-associated background to the scattering from this level has been demonstrated. The peak absorption cross section of 29.7 ± 1.1 barns has been determined from a self-absorption experiment. The self-absorption measurement and a production experiment combine to give values of 64.5 ± 10.4 ev and 59.2 ± 9.7 ev for the total level width and radiative width to the ground state, respectively. The combination of the value of the integrated elastic scattering cross section from the absolute measurement, and those values calculated from the self-absorption and production experiments gives for this integrated cross section the value 2.33 ± 0.19 mb-Mev. The radiation width to the 4.43-Mev state of C^{12} is determined to be 3.2 ± 2.5 ev by fitting the detector resolution function to observed pulse-height spectra. A value for the inelastic scattering in the giant resonance region of C^{12} is determined.

INTRODUCTION

SCATTERED photons from the 15.1-Mev level in C^{12} are easily observed because the scattering cross section of this level is large and it is situated in an energy region that is relatively free of other scattering processes. It is therefore desirable to have available an accurate determination of the parameters of this level for calibration purposes.

Scattering of photons from the 15.1-Mev level in C^{12} was first observed by Fuller, Hayward, and Svantesson at the National Bureau of Standards.[1] The dipole nature of the angular distribution of the scattered photons,[2] and the azimuthal asymmetry about the beam direction resulting from the elastic scattering of a polarized photon beam,[3] serve to determine the spin and parity of the level as (1+). While alpha-particle emission is energetically possible, it is observed to be strongly inhibited.[4,5] This, coupled with the fact that the energy of this level matches the (corrected) energies of the ground states of N^{12} and B^{12}, establishes the level as one of isotopic spin $T=1$.

In the present experiment, angular distribution measurements are extended over a wider angular range than those previously reported, and the result indicates that this is a predominantly dipole transition.

This paper describes a detailed study of the 15.1-Mev level in C^{12}, as excited by bremsstrahlung of maximum energy from 19–42 Mev. The peak absorption cross section of the level, σ_n^0, and the ratio, δ/Γ of thermal Doppler broadening divided by level width are determined by observing the attenuation of the yield of 15.1-Mev photons scattered by a target of fixed thickness, when graphite (or polystyrene) absorbers are placed in the incident bremsstrahlung beam. The thermal Doppler broadening is to be distinguished from the recoil Doppler energy shift, which here amounts to more than 30 kev at 135° to the beam. That the observed attenuation is a function of both δ/Γ and σ_n^0 is easily seen by considering the effect of Doppler broadening on the shape of the assumed cross section, in this case the Breit-Wigner shape. The effect of Doppler broadening is to reduce the effective peak height of the cross section while maintaining the area under the cross section curve constant. This results in a lessened attenuation, for a given σ_n^0, over the case with no broadening. From σ_n^0 and the energy of the level the ratio, Γ_γ/Γ, of the elastic radiative width to the total width can be determined, and the integrated scattering cross section may then be calculated.

A second determination of δ/Γ leading to a value of the integrated cross section is obtained by observing the growth in yield of 15.1-Mev photons as the scatterer thickness is increased.

Finally, the integrated scattering cross section is determined directly by measuring the absolute number of 15.1-Mev photons scattered from a target irradiated by a bremsstrahlung beam of known intensity. This is the only part of the experiment requiring absolute knowledge of beam and detector parameters.

This level parameters which are obtained in this experiment differ from those of a previous experiment,[5] as may be seen by reference to Table I. The major factor in this difference seems to involve the correct subtraction of backgrounds. In particular, this experiment demonstrates that there is a small yield of scattered gamma rays from C^{12} in the range 11–17 Mev. This yield is not strongly affected by absorbers and so will be called the nonresonant contribution to the scattering.

† Research supported by a joint program of the Office of Naval Research and the U. S. Atomic Energy Commission.
* A thesis submitted to the Department of Physics, the University of Chicago, in partial fulfillment of the requirements for the Ph.D. degree.
[1] Fuller, Hayward, and Svantesson, Bull. Am. Phys. Soc. Ser. II **1**, 21 (1956); E. Hayward and E. G. Fuller, Physica **22**, 1138 (1956).
[2] J. E. Leiss and J. M. Wyckoff, Bull. Am. Phys. Soc. Ser. II, **1**, 197 (1956).
[3] P. Axel, Program of the Conference on Photonuclear Reactions held at the National Bureau of Standards, Washington, D. C., April 30, 1958 (unpublished), A.8.
[4] R. W. Kavanagh, Ph.D. dissertation, California Institute of Technology, 1956 (unpublished).
[5] E. Hayward and E. G. Fuller, Phys. Rev. **106**, 991 (1957).

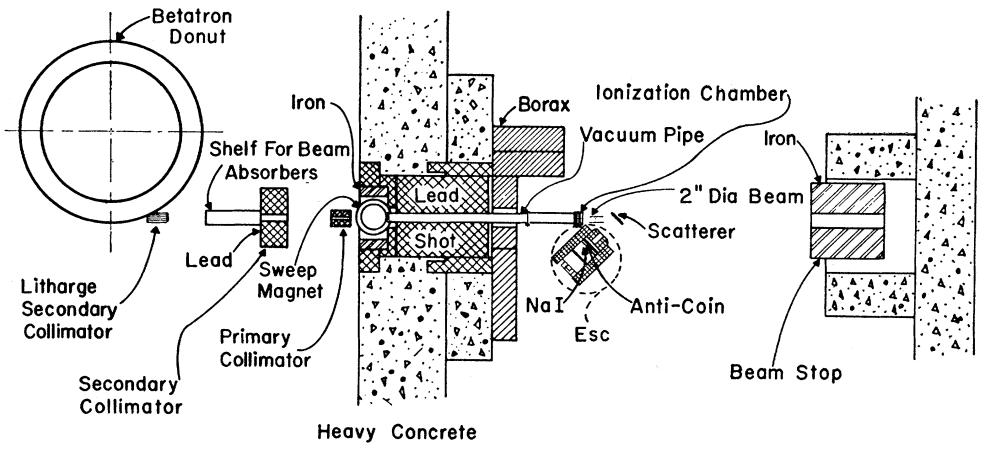

FIG. 1. The experimental arrangement.

EXPERIMENTAL ARRANGEMENT

The arrangement of shielding around the beam area of the University of Chicago 100-Mev betatron is shown in Fig. 1. The iron beam stop prevents low-energy photons and electrons from back-scattering from the back wall into the NaI(Tl) counter. The borax shields the counter from neutrons coming from the main shield wall, while the litharge secondary collimator near the doughnut shields the ionization chamber from bremsstrahlung formed in the doughnut wall instead of on the betatron target (0.010-in. Pt). The sweep magnet (10.75-in. pole diameter, 6000 gauss field) and subsequent vacuum pipe maintain an electron-free beam up to the thin ionization chamber located near the scatterer. The energy-sensitive counter is a 5-in. diam, 4-in. long NaI(Tl) crystal shielded by lead walls 4 in. thick and 16 in. long. Its effective solid angle was determined by a 2.8-in. diam hole in a 5-in. lead collimator placed before it. No radiation shielding was found necessary on either the top or bottom of the counter. The crystal and its phototube were incased in Styrofoam and placed inside a double shield of high permeability magnetic material 12 in. long. An anticoincidence counter ($\frac{1}{8}$-in. plastic scintillator) was placed between the NaI(Tl) crystal and the collimator in order to discriminate electronically against electrons. In addition, 2.16 g/cm^2 of Pb and 4.7 g/cm^2 of Be were placed at the collimator entrance to remove low-energy photons and electrons which would otherwise contribute to pileup in the counter.

The counter was set at 135° to the photon beam for all measurements described in this paper, with the sole exception of the angular distribution determination.

All absorber and scatterer thicknesses considered are measured along the direction of the photon beam, thus eliminating cosine factors from the discussion.

TABLE I. Properties of the 15.1-Mev, $T=1$, $J=1+$ level in C^{12}.

	This experiment	National Bureau of Standards experiment[a]
1. Peak absorption cross section	29.7 ± 1.1	22.2 ± 2.2 barns
2. Ratio of Doppler broadening to total level width	0.62± 0.10	...
3. Total level width	64.5 ±10.4	79 ±16 ev
4. Radiation width to the ground state of C^{12}	59.2 ± 9.7	54.5 ± 9.3 ev
5. Radiation width to the 4.43-Mev state of C^{12}	3.2 ± 2.5	≤5.5 ev
6. Alpha-particle width to the 2.9-Mev state of Be^8	2.1 ± 3.2	($18.6 \leq \Gamma_\alpha \leq 24.5$) ±8.2 ev
7. Integrated elastic scattering cross section	2.33± 0.19	1.90± 0.27 mb-Mev

[a] See reference 5.

ENERGY SCALE

Energy control of the betatron was accomplished by electronically integrating the voltage from a single turn of wire around the betatron pole (flux integrator) and triggering the ejection pulser when the integrated voltage reached a given level. This integrator was calibrated at the 10.83-Mev $Cu^{63}(\gamma,n)Cu^{62}$ threshold,[6] and by suitably calculating the correction for the delay in emergence of x-rays after the trigger pulse, furnished an energy scale for the machine. This delay correction takes into account the gain in energy of the circulating electron beam due to the fact that the betatron field continues to increase in magnitude in the interval between the triggering of the ejection pulser and the emergence of x-rays. The energy scale was also checked by an absolute energy measurement obtained by integrating the output of a small search coil of known parameters, located at the target radius, and measuring the integrated voltage at the time of emergence of x-rays. The agreement between the two energy scales over the range 19–42 Mev was within 2% which was adequate for this experiment.

MONITORING

All runs were monitored in terms of the charge collected from the thin (total thickness 0.004-in. Fe,

[6] Quisenberry, Scolman, and Nier, Phys. Rev. **104**, 461 (1956).

0.006-in. Al) three-plate transmission ionization chamber shown in Fig. 1. This charge was collected on a polystyrene capacitor and read by an Applied Physics Corporation model 30L vibrating reed electrometer.

The ionization chamber was originally located immediately after the primary collimator, but it was then observed that the chamber was sensitive to low-energy radiation sprayed backward from the inside of the betatron main shield wall. The chamber was therefore placed outside the main shield wall at the end of the vacuum pipe. Absorbers are placed on the shelf before the lead secondary collimator shown in Fig. 1. Although the ionization chamber actually is located in the beam after the absorbers, it is convenient to transform the chamber readings to the values they would have if the chamber were located in a collimated beam before the absorbers. The factors required for the above transformation are empirically measured for the various absorber thicknesses at each betatron energy employed.

Since this paper is concerned only with the specifically nuclear nature of photon absorption and scattering at 15.1 Mev, it is convenient to calculate the attenuation of photons of this energy by electronic processes (photoelectric effect, Compton scattering, and pair production) in the absorbers,[7] and to reduce the transformed ionization chamber reading by the amount of this calculated attenuation. This procedure gives a corrected ionization chamber reading which corresponds, for each absorber thickness, to the number of photons (in a one-Mev bin centered at 15.1 Mev) incident on the scatterer, assuming that the nuclear absorption in the absorber has no effect on this number. (For this case, the nuclear absorption is less than 1% of the electronic absorption, when averaged over a one-Mev bin.)

To obtain the absolute number of 15.1-Mev photons in the beam, the thin chamber was compared in the same bremsstrahlung beam with a thick ionization chamber of the Kerst-Edwards type[8] which had been calibrated calorimetrically at the National Bureau of Standards. The calibration is in terms of energy in the incident beam emerging through a given doughnut thickness in units of Mev per coulomb collected from the chamber, as a function of bremsstrahlung energy. At the Chicago betatron, the beam emerges through the same doughnut thickness as at the National Bureau of Standards, and no correction need be made for the effect of the doughnut, although with a different machine this might not be so. To determine the number of photons (in a one-Mev bin centered at 15.1 Mev) in the beam for a given charge collected from the Kerst-Edwards type chamber, the number of Mev in the beam is calculated from the calibration of the chamber, and multiplied by a factor obtained from a tabulation of the Schiff spectrum[9] for the given machine operating energy. To check that the bremsstrahlung spectrum from this machine was not grossly distorted, the $Cu^{63}(\gamma,n)Cu^{62}$ yield curve was constructed by applying the bremsstrahlung tables[9] to the averaged curve obtained from the values of this cross section[10] reported by many laboratories. An experimental yield point was obtained by absolute β^+ counting and the comparison between this point and the yield curve above was used to infer the energy in the beam, per coulomb collected from the Kerst-Edwards type chamber. This value agreed with the National Bureau of Standards calibration within the $\pm 10\%$ estimated error on the β^+ counting.

Because, in the past, values of cross sections determined at various machines have varied by about $\pm 10\%$ for reasons not well understood, an error of $\pm 10\%$ is assigned to the knowledge of the absolute beam intensity at this betatron.

ELECTRONIC PULSE PROCESSING

The main features of the electronic equipment[11] employed in this experiment are shown in Fig. 2. The current pulses from the Dumont type 6364 photomultiplier are integrated at the grid of cathode follower 1. The differentiator in the fast branch of the circuit delivers a prompt pulse proportional to the ultimate height of the integrated pulse passed by the slow branch of the circuit. The anticoincidence circuit produces an output pulse (only in the absence of a charged particle pulse) which may be transmitted by the betatron beam gate and used to trigger the linear gate. The pulse can pass through the betatron beam gate only during a time encompassing the betatron beam pulse. This reduces the cosmic-ray background by the duty cycle of the betatron beam gate. Pulses which pass through the linear gate are presented to the 50-channel pulse-height analyzer for analysis. The threshold above which pulses are analyzed is set by the step attenuator in the fast branch of the circuit.

Should the pulse exceed channel 50 in the analyzer, it does not appear in the memory or memory totalizer, but instead on the over-bound scaler. The analyzer circuitry is so arranged that only one pulse per betatron burst may be accepted. To quantitatively reconstruct the pulse-height spectrum, the spectrum in the analyzer is multiplied by the ratio of the difference of counts in the gate and over-bound scalers to the number of counts in the memory totalizer. The threshold for pulse processing is always adjusted (in the fast branch) so that the low-energy cutoff of the spectrum is well above channel one in the analyzer, guaranteeing that no pulses are lost due to thresholds set in its internal circuits. The

[7] G. R. White, National Bureau of Standards Report, NBS-1003, 1952 (unpublished).
[8] P. D. Edwards and D. W. Kerst, Rev. Sci. Instr. 24, 490 (1953).
[9] A. S. Penfold and J. E. Leiss, "Bremsstrahlung Tables," University of Illinois Report (unpublished).
[10] From a compilation by A. S. Penfold (private communication).
[11] A more detailed description of the equipment will be published separately.

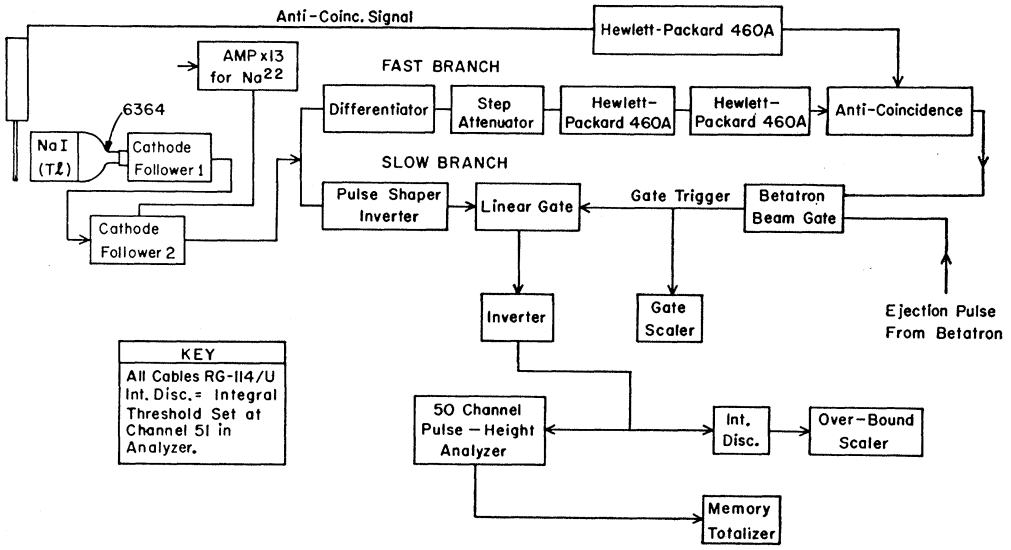

FIG. 2. Electronics block diagram.

differential linearity of the system was determined to be constant to about 1%, from channel 10–50.

The equipment had a parallel branch from the output of cathode follower 1 to the anticoincidence circuit on the fast side, and to the linear gate on the slow side. Pileup checks were performed by feeding this parallel branch from a pulser triggered at the peak of the betatron photon pulse, and triggering the linear gate only on pulser pulses. Since pulser and phototube pulses were added at the linear gate, the resulting pulse-height spectrum yielded a direct measure of pileup at the given beam intensity. Throughout this experiment, the maximum pileup tolerated was a broadening of $\pm\frac{1}{2}$ channel. No gross shift of pulser peak position occurred because the pulses from the pulse shaper were bipolar.

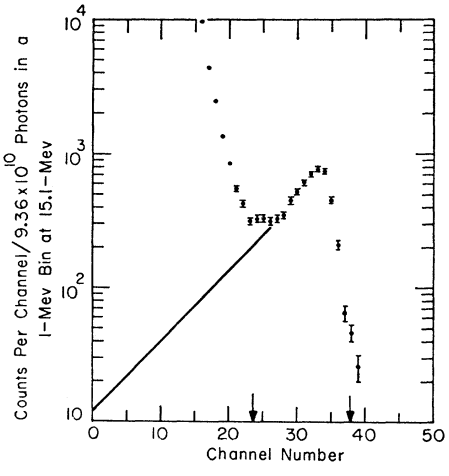

FIG. 3. The pulse-height spectrum produced in the NaI(Tl) crystal at 135° to the beam, when a 0.483-g/cm² polystyrene scatterer is irradiated in a 42-Mev bremsstrahlung beam for 110 minutes. The solid line indicates the extrapolation used to obtain the total number of interactions produced in the crystal by 15.1-Mev photons. The region between the two arrows is that region over which the distribution is summed. The factor relating photon energy and pulse-height analyzer channel number is 0.45 Mev/channel.

PHOTOMULTIPLIER GAIN

In order to monitor the gain of the photomultiplier, a spectrum of a radioactive source (Na^{22}) was taken by connecting cathode follower 1 to the amplifier shown in Fig. 2. The position of this peak (11% wide at half-height) coincided exactly in the analyzer with the position of the 15.1-Mev peak observed in the experiment. The position of the Na^{22} peak was determined immediately before and after each run, and the average taken to indicate the position during the run. The largest variation in Na^{22} peak position over a run was observed to be 2%. The betatron was always operated for about 10 mintues at the intensity to be used during the run before taking a Na^{22} spectrum. This procedure was necessary because an increase (5% maximum) in gain of the photomultiplier with high counting rate was observed. After the beam was shut off, the gain decayed to its original value with about a 10 minute half-life, allowing ample time to make the half-minute Na^{22} peak positioning run without any significant change in gain.

A TYPICAL PULSE-HEIGHT SPECTRUM

A typical pulse-height spectrum for the 15.1-Mev C^{12} level, corrected for counting losses, is shown as a semi-logarithmic plot in Fig. 3. This spectrum was obtained by irradiating a 0.483-g/cm² polystyrene scatterer (0.342 g/cm² at 45° to the beam) for 110 minutes in a 42-Mev bremsstrahlung beam. The counter was at the usual 135°. The solid line in the figure shows the extrapolation used to obtain the total number of interactions in the crystal due to the 15.1-Mev level. The sharp edge in the spectrum near channel 20 can be

ascribed to photons, for the attenuation in the spectrum measured by placing lead absorber before the counter collimator agrees with the calculated attenuation in lead for photons of energy corresponding to the position of the rise in the spectrum. The two arrows indicate the region over which the spectrum is summed for subsequent analyses. The flat valley at about channel 24 corresponds to transitions to the first excited state of C^{12} at 4.43-Mev.

BACKGROUNDS

In this experiment, there are three backgrounds contributing to the summation interval of Fig. 3: cosmic-ray background, beam-induced scatterer-out background, and the so-called nonresonant contribution.

The cosmic-ray backgrounds as determined by applying the calculated betatron gate duty cycle to an ungated cosmic-ray spectrum, or by pulsing the betatron gate with the beam off and observing the resulting spectrum, are found to agree. The cosmic-ray contribution to the spectrum of Fig. 3, for instance, is essentially flat over the interval of summation, and amounts to about 6 counts per channel.

The scatterer-out background at 135° to the photon beam and with 42-Mev bremsstrahlung is essentially flat from channel 38 to channel 23. Below channel 23 it follows the spectrum of Fig. 3 but is a factor of three lower. The contribution of the scatterer-out background over the region of summation is about 21 counts per channel in Fig. 3. The scatterer-out background was determined for each absorber thickness and energy. These measurements show that some of this background is due to radiation leakage through the betatron shield wall.

The nonresonant contribution is about 61 counts per channel over the summation interval of Fig. 3.

Henceforward, it shall be assumed in all discussions that the known cosmic-ray and scatterer-out backgrounds have been subtracted from the observed yields, and that all yields are corrected for counting losses. All yields are normalized to a fixed number of photons (in a one-Mev bin centered at 15.1 Mev) incident on the scatterer.

THE ANGULAR DISTRIBUTION

The angular distribution of photons scattered from the 15.1-Mev level in C^{12} has been measured by a difference technique made possible by the fact that the nuclear absorption of 15.1-Mev photons in 6 g/cm² graphite is 83%, while electronic absorption is only 10%. Figure 4 shows the difference of yield of counts in the summation interval with no absorber in the beam, and with about 6 g/cm² of graphite in the beam plotted for the various angles of observation. All effects of electronic absorption in the 0.483-g/cm² polystyrene target are calculated away. The plotted difference is therefore due to nuclear scattering. For reference,

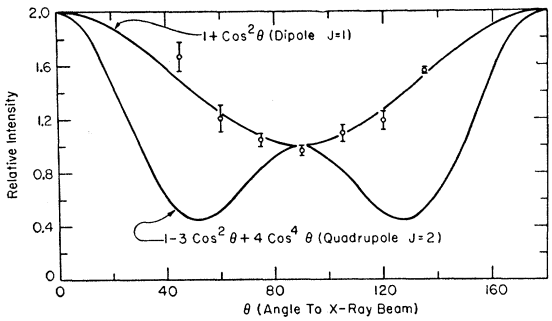

FIG. 4. The angular distribution of photons scattered from the 15.1-Mev level in C^{12}.

Fig. 4 shows the angular distributions expected for dipole $J=1$ and quadrupole $J=2$ transitions. It is apparent that the transition is dipole.

THE NONRESONANT CONTRIBUTION TO THE SCATTERING

The width of the peak in the pulse-height distribution shown in Fig. 3 is principally due to the response of the NaI counter to the photons scattered from the 15.1-Mev level in C^{12}. All calculations of the parameters of this level were based on a summation of the counts taken over the region between the arrows in Fig. 3. It was experimentally demonstrated that not all of the counts in the summation region were due to scattering from the 15.1-Mev level, and that this was true not only for 42-Mev bremsstrahlung (as in Fig. 3) but for all energies at least down to 19 Mev.

This extraneous yield is called the nonresonant contribution to the scattering (NRC), since it is not strongly affected by carbon absorbers placed in the main beam, and it increases linearly with the thickness of the scatterer.

If the channel by channel differences of the pulse-height spectra from a target without and with absorber in the beam be formed, the result is the resolution function for the resonant level only. The resolution function so obtained was checked by performing such subtractions for many sets of absorber-in absorber-out runs. The resolution function obtained by the subtraction process was narrower than the peaks in the spectra. This indicated the presence of some nonresonant scattering. The addition of counts (uniform over the summation region) to the resolution function gave a good fit to the pulse-height spectra for all values of beam absorber. Thus the NRC to the sum could be determined.

Figure 5 indicates the contributions of the NRC to the summation interval obtained from resolution function fitting (for irradiation of a 0.483-g/cm² polystyrene scatterer in a 42-Mev bremsstrahlung beam, per 1.04 $\times 10^{10}$ photons in a one-Mev bin at 15.1 Mev). Since the contribution is constant as a function of absorber thickness, the nonresonant nature is demonstrated,

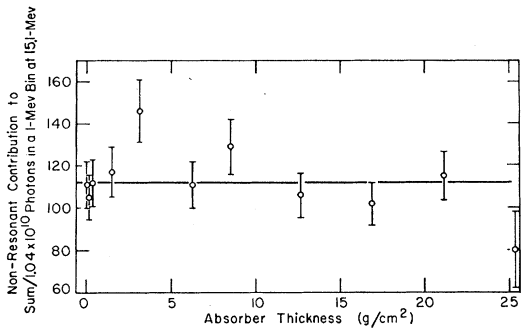

FIG. 5. The nonresonant contribution to the interval of summation, *versus* absorber thickness for which the contribution was determined by fitting the resolution function to the observed pulse-height spectrum. Scatterer, beam energy, and detection angle were as for Fig. 3.

i.e., it absorbs like the electronic processes at energies near 15 Mev.

A byproduct of the determination of the NaI resolution function was the branching ratio for transitions from the 15.1-Mev level to the first excited state at 4.43 Mev, and to the ground state. The branching ratio is found to be 0.05 ± 0.04, consistent with determinations of 0.095 ± 0.014 by Waddell[12] and <0.10 by Fuller and Hayward.[5]

When the number of g/cm^2 of C^{12} in the scatterer was increased by a factor of 13.6, the NRC increased by a factor 12.4 from 112 ± 10 to 1380 ± 136. Since the electronic absorption in the thicker scatterer is about 8%, this demonstrates that the NRC is not self-absorbed by the scatterer.

Figure 9 shows theoretical curves for the attenuation of the 15.1-Mev photons as a function of absorber thickness. (The derivation of these curves is discussed in the section on the self-absorption experiment.) It can be seen that for thick enough absorbers the curves are concurrent, independent of the parameter t. By assuming a reasonable value for $\sigma_n{}^0$ (obtained by approximately fitting experimental points for thin absorbers), an estimate of the photon attenuation due to the resonant level at large absorber thicknesses can be made. For example, assuming $\sigma_n{}^0=30$ barns and a graphite absorber of 26.1 g/cm^2, the curves imply that 5.9% of the original 15.1-Mev photons should remain. Experimentally, it is found that 19.8% remain at this absorber thickness. The difference may be attributed to the NRC.[13] Calculation shows this 13.9% difference corresponds to an NRC of 109 ± 5 for the conditions of target, photon dose, and bremsstrahlung energy of Fig. 5. It is seen that this value is consistent with the measurements of NRC from spectral shape fitting. It is of interest to note that without removal of approximately the above amount of NRC, the experimental points fit none of the theoretical curves of Fig. 9. The NRC shall be taken as 109 ± 5 under the conditions prevailing in Fig. 5. This is close to the average value of 112 shown in Fig. 5, and within the error on that average.

The NRC was determined as a function of bremsstrahlung energy in a manner which will now be described. Let the yield from a scatterer in the 42-Mev strahlung beam with no absorber in the beam, $Y(0,42)$ and with graphite absorber in the beam, $Y(T,42)$, be determined. Since the value of NRC at 42 Mev, $B(42)$, is known, a value of the ratio, R, of pure resonant yields without and with absorber may be calculated:

$$R=[Y(0,42)-B(42)]/[Y(T,42)-B(42)]. \quad (1)$$

This ratio does not change as the bremsstrahlung energy is varied so the NRC for bremsstrahlung energy E_0, $B(E_0)$, could be determined by measuring only $Y(0,E_0)$ and $Y(T,E_0)$:

$$B(E_0)=[RY(T,E_0)-Y(0,E_0)]/[R-1]. \quad (2)$$

Figure 6 is a plot of $B(E_0)$ for a 0.483-g/cm^2 polystyrene scatter (per 1.04×10^{10} incident photons in a one-Mev bin centered at 15.1 Mev) *versus* maximum energy of the incident bremsstrahlung beam. The horizontal lines indicating the smaller errors on each point were derived assuming $B(42)=109\pm0$, while the lines indicating the larger errors on each point were calculated assuming $B(42)=109\pm5$ and show the systematic displacement (all points shift up or down together) introduced under the latter assumption.

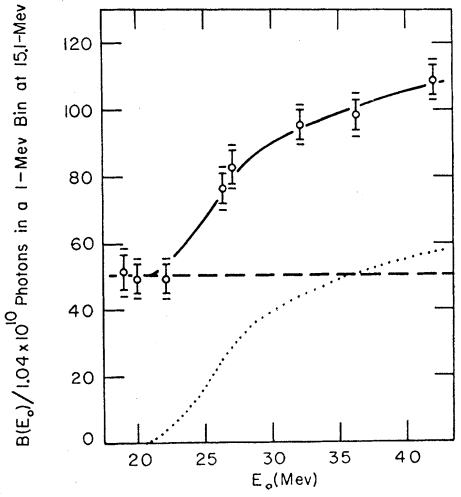

FIG. 6. The nonresonant contribution to the interval of summation, *versus* betatron energy. Scatterer, beam energy, and detection angle were as for Fig. 3.

[12] C. N. Waddell, University of California Radiation Laboratory Report UCRL-3901, 1957 (unpublished).

[13] It is not difficult to calculate the upper limit of scattering into a bin of width ϵ at 15.1 Mev, due to Compton processes in the absorber. For the geometry of this experiment, $\theta_{max}=1.2°$. $h(\nu_0-\nu)=h\nu h\nu_0(1-\cos\theta)/mc^2$, so $h(\nu_0-\nu)=0.14$ Mev. The differential cross section for Compton scattering into a bin of width ϵ Mev is $6.5\epsilon\times10^{-4}$ barns. For 100 g/cm^2 of graphite absorber there are 3×10^{25} electrons/cm^2, so the ratio of the number of photons scattered into ϵ to the number originally in the bremsstrahlung bean is $N/N_0=6.5\epsilon\times10^{-28}\times3\times10^{25}\times0.14/\epsilon=2.7\times10^{-3}$, assuming no re-absorption of the scattered photons. This process is therefore negligible in the experiment.

The uniformly dashed horizontal line corresponds to NRC from levels near 15.1 Mev, while the dotted curve corresponds to NRC from levels assumed to have the shape of the $C^{12}(\gamma,n)$ giant resonance.[14] This curve is calculated from the bremsstrahlung tables,[9] and normalized to constant 15.1-Mev photon flux. These curves have been normalized to give the best fit to the data points. The solid curve is the sum of the dotted and the dashed curve. It is seen that the data points are consistent with this decomposition of the NRC.

The dashed curve corresponds to an integrated cross section of 0.10 mb-Mev due to levels near 15 Mev, while the dotted curve corresponds to an integrated cross section of 0.21 mb-Mev arising from levels in the giant resonance leading to the emission of 11–18 Mev photons. These values are based on the integrated scattering cross section for the 15.1-Mev level of 2.33 mb-Mev, from Table I.

The point on Fig. 6 at $E_0=20$ Mev was directly checked by an attenuation measurement and reference to the curves of Fig. 9, as discussed earlier. The value of NRC so obtained was 45 ± 8, which is consistent with the value in Fig. 6.

To demonstrate that the correct NRC was indeed determined, the total yield of counts in the summation interval was measured as a function of betatron energy. The upper set of points in Fig. 7 is the yield from a 5.98-g/cm² graphite scatterer at various betatron energies, while the lower set of points is derived from the upper set by subtracting the NRC of Fig. 6, multiplied by a factor 12.7 to correct for the increased thickness and electronic absorption of this scatterer. The expected yield from the 15.1-Mev level appears as the solid curve in Fig. 7. This curve is normalized to make a best fit with the lower set of points. The upper

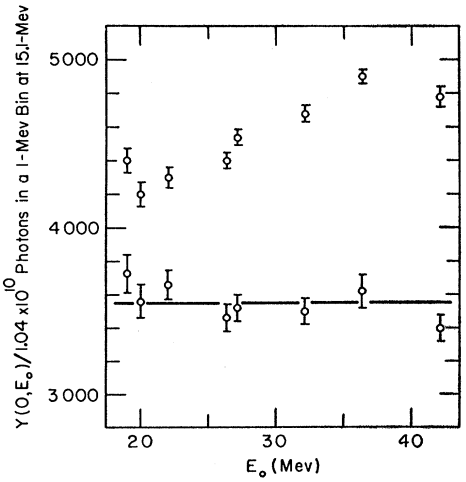

FIG. 7. Yield from a 5.98-g/cm² scatterer as a function of betatron energy. The upper points are raw data. The lower points have had the appropriate nonresonant contribution (NRC) subtracted.

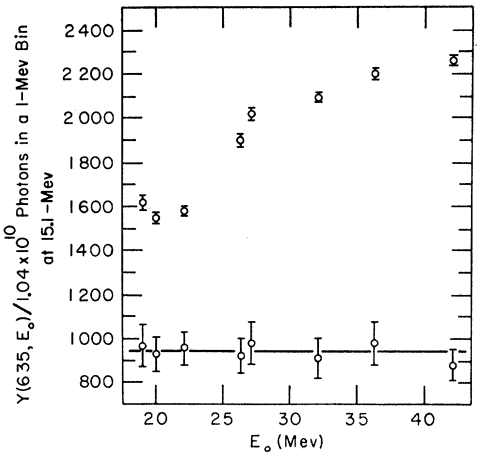

FIG. 8. Yield from a 5.98-g/cm² scatterer with 6.35-g/cm² absorber in the incident beam as a function of betatron energy. The upper and lower sets of points have the same significance as in Fig. 7.

set of points in Fig. 8 is the yield from the scatterer of Fig. 7 with 6.35 g/cm² graphite absorber in the incident beam. The lower set of points is obtained from the upper set as in Fig. 7. In both these figures the original data points do not fit a horizontal line, while the final points fit such a line well. This is regarded as a good test of the correctness of the NRC of Fig. 6. Henceforth, it shall be assumed that the NRC has been subtracted from all yields under discussion.

THE SELF-ABSORPTION EXPERIMENT

The self-absorption experiment consisted in observing the attenuation in the number of photons scattered by 135° from a polystyrene target in a 42-Mev bremsstrahlung beam, as a function of the thickness of absorber placed in the incident beam.

The nuclear cross section, $\sigma_n(E)$, is assumed to be given by folding a Gaussian distribution for the thermal motions of the scatterer nuclei into the Breit-Wigner one-level formula[15]:

$$\sigma_n(E)=\sigma_n{}^0\frac{1}{2(\pi t)^{\frac{1}{2}}}\int\frac{\exp[-(x-y)^2/4t]}{1+y^2}dy, \qquad (3)$$

where: $x=2(E-E_0)/\Gamma$, $t=(\delta/\Gamma)^2$. $\sigma_n{}^0$, E_0, E, Γ, and δ are the peak absorption cross section at exact resonance, the resonance energy, the actual energy, the full level width at half-maximum, and the "Doppler width," respectively. For photons of energy E incident on a nucleus of mass M, the Doppler width may be given by

$$\delta=E[2kT'/Mc^2]^{\frac{1}{2}}, \qquad (4)$$

where k is the Boltzmann constant, c is the velocity of light, and T' is an effective temperature which takes account of the vibration of the scatterer atoms

[14] B. C. Cook, Phys. Rev. **106**, 300 (1957).

[15] H. A. Bethe, Revs. Modern Phys. **9**, 71 (1937), Sec. 61.

due to their binding in a chemical lattice.[16] The value $T'=456°K$ is obtained for graphite from the graph of T'/T *versus* T/θ in the article by Lamb by assigning a value[17] of 1000°K to the Debye temperature θ. Thus, the value of δ obtained for graphite from (4) is $\delta=40$ ev. This value of δ is assumed to be correct for both polystyrene and graphite, since it has been shown in a previous experiment[5] and verified in this laboratory that graphite and polystyrene can be permuted as scatterer and incident beam absorber, with no effect on the observed nuclear absorption. Also, on theoretical grounds, Montroll[18] has stated that the mean energy of carbon atoms in these materials will be determined chiefly by the presence of the carbon-carbon bond, so that the Doppler widths for these materials are expected to be nearly equal.

The yield of scattered photons, $Y(\Delta)$, from a scatterer whose thickness in the direction of the incident beam is T, with absorber of thickness Δ in the incident beam is

$$Y(\Delta)=C\int e^{-\sigma_n(E)\Delta}[1-e^{-\sigma_n(E)T}]dE, \qquad (5)$$

where C is a constant of proportionality and the effects of electronic absorption processes (less than 1%) in the scatterer are neglected. In this case, the level width is some 500 times less than the recoil Doppler shift, so that nuclear re-absorption in the scatterer does not occur. The effect of electronic absorption in the absorber on (5) has been removed as described in the section on "Monitoring."

In order to put (5) in a form which does not involve T, construct:

$$Y(\Delta-\tfrac{1}{2}T)=C\int e^{-\sigma_n(E)\Delta}\sigma_n(E)T \times\left[1+\frac{[\sigma_n(E)T]^2}{24}+\cdots\right]dE. \qquad (6)$$

Assuming the values of level parameters stated in the conclusions, and taking into account the effective reduction of about a factor two in $\sigma_n{}^0$ due to Doppler broadening,[19] the value of $[\sigma_n(E_0)T]^2/24$ for the 0.483 g/cm² polystyrene scatterer used is 7×10^{-3}. To the accuracy required in the experiment, this quantity is negligible, so that:

$$Y(\Delta-\tfrac{1}{2}T)/Y(-\tfrac{1}{2}T) \approx W(\Delta)\equiv\int e^{-\sigma_n(E)\Delta}\sigma_n(E)dE\Big/\int\sigma_n(E)dE. \qquad (7)$$

The right-hand side of (7) is independent of T, and has the further property that it is expressible solely as a function of the product $\sigma_n(E)\Delta$. The data give values of $Y(\Delta)$, so that when $Y(-\frac{1}{2}T)$ is determined, the left-hand side of (7) is obtained from the data. The procedure for obtaining $Y(-\frac{1}{2}T)$ from the data will be described.

Calculations of the right-hand side of (7) for various values of $t=(\delta/\Gamma)^2$ were kindly carried out by E. Hayward and E. G. Fuller on a computer at the National Bureau of Standards and sent to this laboratory. The theoretical curves obtained from these calculated points are shown in Fig. 9. These curves are universal in the sense that they do not depend implicitly on $\sigma_n{}^0$ or on target thickness for a sufficiently thin target.

It is observed for all values of t that plots of $\log W(\Delta)$ *versus* $\sigma_n{}^0\Delta$ are straight lines for $\sigma_n{}^0\Delta<1.35$. The value of $Y(-\frac{1}{2}T)$, needed to construct the left-hand side of (7), corresponds to the yield for a scatterer of thickness T, but which has no self-absorption of photons, i.e., it only scatters. $Y(-\frac{1}{2}T)$ is found by performing a least-squares fit to a straight line of $\log Y(\Delta)$ *versus* $\sigma_n{}^0\Delta$ for the first 13 data points, corresponding to $\sigma_n{}^0\Delta<1.35$. The extrapolation of this line then yields $Y(-\frac{1}{2}T)$, and the data may be put in the form $W(\Delta)$ *versus* Δ. The data are plotted in Fig. 9 with the value of $\sigma_n{}^0$ assumed to be 29.7 barns, obtained from the results of the fitting procedure which will now be described. (The first point plotted corresponds to $\Delta=0.248$ g/cm², and the last to $\Delta=49.2$ g/cm².)

The fit of the data to the theoretical curves was determined by the following method, described for only *one of the curves* of the family in Fig. 9. The value of $W(\Delta)$ belonging to a given datum point was located in the curve in Fig. 9. The value of $\sigma_n{}^0\Delta$ at this point on the curve was read off the abscissa, as were the value of $\sigma_n{}^0\Delta$ corresponding to the extremes of the statistical

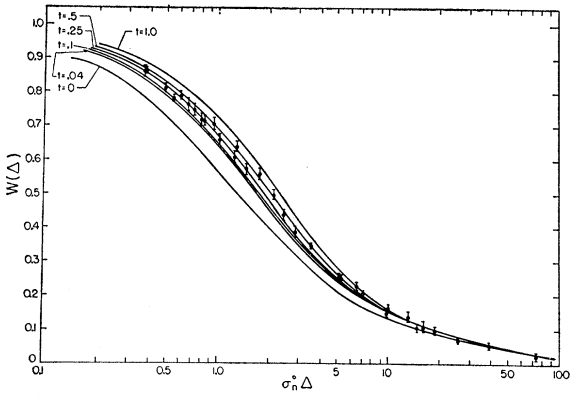

FIG. 9. Theoretical attenuation curves for a Doppler-broadened Breit-Wigner level. The abscissa is the product of the peak absorption cross section and the effective absorber thickness. The individual curves correspond to the marked values of $t=(\delta/\Gamma)^2$. The points plotted are the self-absorption data with the non-resonant contribution subtracted, assuming $\sigma_n{}^0=29.7$ barns.

[16] W. E. Lamb, Jr., Phys. Rev. **55**, 190 (1938).
[17] W. De Sorbo and W. W. Tyler, J. Chem. Phys. **21**, 1660 (1953); J. Krumhansl and H. Brooks, J. Chem. Phys. **21**, 1663 (1953).
[18] E. Montroll (private communication).
[19] James Rainwater, *Handbuch der Physik*, edited by S. Flügge (Springer-Verlag, Berlin, 1957), Vol. 40, pp. 377–381.

error on $W(\Delta)$ for that datum point. These values of $\sigma_n{}^0\Delta$ were then divided by the known Δ for the point to render a value for $\sigma_n{}^0$, with errors, corresponding to that one datum point. This procedure was then repeated for all other data points, and a mean value for $\sigma_n{}^0$, $\bar{\sigma}_n{}^0$, weighted according to the reciprocal of the square of the error on each point, was constructed. This is shown in Fig. 10 for several values of δ/T. For the curve in Fig. 9 corresponding to the true level parameters, the $\sigma_n{}^0$ determined should be constant for all data points, if there were no errors. The spread of values of the individual $\sigma_n{}^0$ about $\bar{\sigma}_n{}^0$ was expressed by calculating χ^2. This χ^2 calculation was repeated for each of the curves of Fig. 9. The position of the minimum in χ^2 was taken to indicate the best fit of data to theory. Figure 11 shows the values of χ^2 obtained for the fit to the 32 data points, plotted against δ/Γ, with a parabola fitted to the points. The $\delta/\Gamma=0$ point is not fitted to the parabola because it is quite far from the minimum. The errors indicated in Fig. 11 are due to the contributions to χ^2 arising from inaccuracies in reading Fig. 9. The standard deviation of the measurement is indicated by arrows on Fig. 10 and Fig. 11, and is given by those values of δ/Γ at which χ^2 is one greater than the value of χ^2 at the minimum. The value obtained is seen to be $\delta/\Gamma=0.59\pm0.12$ from Fig. 11. As seen in Fig. 10, this implies a value for $\bar{\sigma}_n{}^0$ of 29.7 ± 1.1 barns.

For a dipole transition Γ_γ/Γ is given by $\sigma_n{}^0/6\pi\lambda\!\!\!^{-2}$, so the value $\bar{\sigma}_n{}^0=29.7\pm1.1$ barns implies $\Gamma_\gamma/\Gamma=0.92\pm0.034$. From the value of $\delta/\Gamma=0.59\pm0.12$ coupled with the previously discussed value of $\delta=40$ ev, Γ is determined to be 67 ± 14 ev. Γ_γ/Γ and Γ combine to determine $\Gamma_\gamma=62\pm11$ ev, where the correlation between Γ_γ/Γ and Γ indicated by Fig. 10 is taken into account in determining the error. It is to be noted that both Γ_γ and Γ are directly proportional to δ, and a systematic error in estimating it directly affects them, as well as the calculated value for the integrated scattering cross section discussed below.

The integrated scattering cross section, I, may be expressed as

$$I=\int\sigma_s(E)dE=\tfrac{1}{2}\pi\Gamma_\gamma\sigma_n{}^0, \tag{8}$$

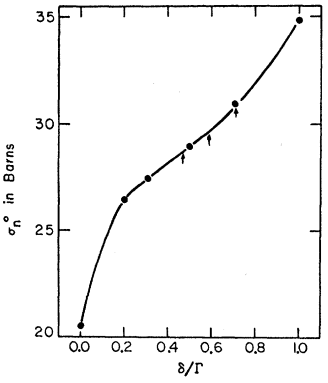

FIG. 10. The weighted mean of the peak cross section of the level determined from the self-absorption data for each of the theoretical curves of Fig. 9.

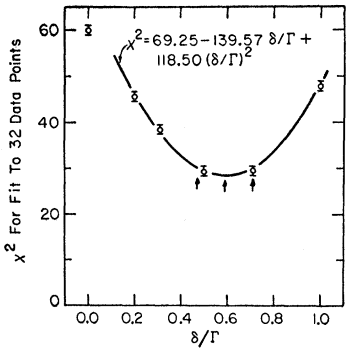

FIG. 11. χ^2 obtained from the data, for each of the theoretical curves of Fig. 9. The parabola is least-squares fitted to the points (except $\delta/\Gamma=0$). The mean and standard deviation of the measurement are indicated by arrows.

where $\sigma_s(E)$ is the scattering cross section, and is $\sigma_n(E)\Gamma_\gamma/\Gamma$. I may be calculated from the parameters determined in the self-absorption experiment to be 2.92 ± 0.41 mb-Mev, with the correlation between $\sigma_n{}^0$ and Γ_γ taken into account in determining the error estimated.

THE PRODUCTION EXPERIMENT

The production experiment consisted in studying the growth in the number of 15.1-Mev photons as a function of scatterer thickness. The bremsstrahlung energy was 42 Mev, and the counter was set at 135° to the photon beam. It is assumed that the nonresonant contribution is subtracted in the yield under discussion.

The yield, $A(T)$, of scattered photons from a scatterer of thickness T in the direction of the photon beam is given by (5), with $\Delta=0$:

$$A(T)=C\int[1-e^{-\sigma_n(E)T}]dE. \tag{9}$$

Curves of $\log A(T)/\delta$ *vs* $\log(T\sigma_n{}^0\Gamma/\delta)$ for various δ/Γ are available.[19] If $\bar{\sigma}_n{}^0$ is taken to be 29.7 barns from the self-absorption measurement, the data points may be fitted to the various curves, and a value of χ^2 for the fit to each of the curves may be plotted as a function of δ/Γ. The data points, corrected for electronic absorption in the scatterer and with the nonresonant contribution subtracted, are plotted in Fig. 12. The solid curve is the theoretical curve for $\delta/\Gamma=0.7$. Figure 13 is a plot of the values of χ^2 *versus* δ/Γ, fitted to a parabola to obtain the minimum. The value obtained from this measurement is $\delta/\Gamma=0.67\pm0.16$, which is consistent with the value $\delta/\Gamma=0.59\pm0.12$ obtained from the self-absorption experiment, and is nearly independent of that experiment; i.e., changing $\bar{\sigma}_n{}^0$ by ±1 barn does not affect the position of this minimum in χ^2.

Using the value of $\delta=40$ ev previously discussed, from this experiment a total level width of 60 ± 15 ev is obtained. The value $I=2.56\pm0.16$ mb-Mev for the integral scattering cross section (8), is obtained from this Γ and the $\sigma_n{}^0$ from the self-absorption experiment. Both I and Γ are proportional to the value of δ assumed, as was the case in the self-absorption measurement.

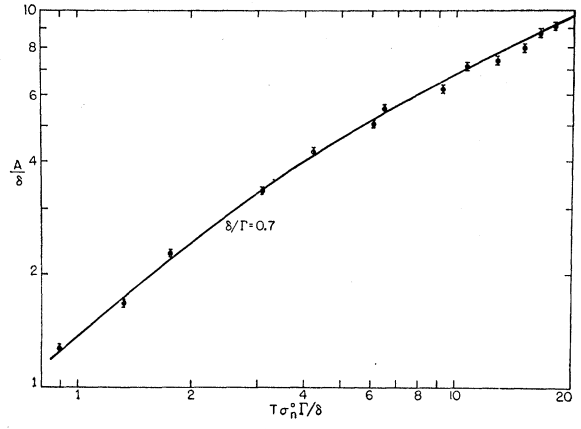

FIG. 12. One theoretical production curve for a Doppler-broadened Breit-Wigner level, corresponding to $\delta/\Gamma=0.7$. The points are the production data less the nonresonant contribution, plotted assuming $\sigma_n^0=29.7$ barns.

THE INTEGRATED SCATTERING CROSS SECTION

The number of photons, S, scattered from a target of thickness T (in which electronic absorption is a negligible process) is given by

$$S=\frac{\Delta\Omega}{11.2}n(15.1)\frac{\Gamma_\gamma}{\Gamma}\int[1-e^{-\sigma_n(E)T}]dE, \qquad (10)$$

where $\Delta\Omega$ is the effective solid angle for detecting a 15.1-Mev photon scattered at 135°; the number 11.2 is the ratio of the total cross section to the differential cross section at 135° for an angular distribution of the form $(1+\cos^2\theta)$; and $n(15.1)$ is the number of photons in a one-Mev bin at 15.1 Mev incident on the scatterer. Denoting the number of scattered photons in the absence of self-absorption by S', (10) becomes

$$S'=\frac{\Delta\Omega}{11.2}n(15.1)T\int\sigma_s(E)dE, \qquad (11)$$

which explicitly contains the integrated scattering cross section, I, defined in (8). Rearranging (11), one obtains

$$I=11.2S'/[\Delta\Omega n(15.1)T]. \qquad (12)$$

Thus, measurement of I requires the determination of S', $\Delta\Omega$, and $n(15.1)$.

In the discussion of the absorption experiment, it was demonstrated that $Y(-\frac{1}{2}T)$, the yield from a scatterer

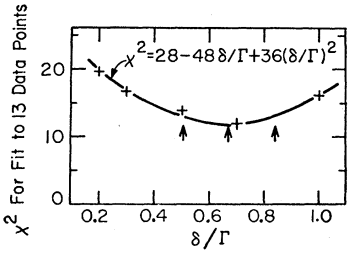

FIG. 13. χ^2 obtained from fitting the data to the production curves for the values of δ/Γ indicated. The points have been fitted to a parabola. The mean and standard deviation of the measurement are indicated by arrows.

of thickness T but with no self-absorption, could be obtained. Since the same scatterer was employed in this experiment as in the self-absorption experiment, the value of $Y(-\frac{1}{2}T)$ may be taken from that experiment to be 726 ± 7.7, for $n(15.1)=(1.04\pm0.10)\times10^{10}$ photons in a one-Mev bin, centered at 15.1 Mev.

The effective solid angle, $\Delta\Omega$, is 10% larger than the geometrical solid angle due to the fact that not all photons are stopped by the lead collimator in front of the NaI crystal. Numerical integration gives 0.0359 stearadian for $\Delta\Omega$.

From the extrapolation in Fig. 3, it is found that $(75\pm8)\%$ of the interactions from 15.1-Mev photons occurring in the NaI crystal lie within the interval of summation, and that the contribution to the summation of transitions from the 15.1-Mev level to the 4.43-Mev first excited state of C^{12} amount to $(2.4\pm2)\%$. To determine the absolute number of interactions in the crystal, $Y(-\frac{1}{2}T)$ must therefore be multiplied by 1.30 ± 0.14.

It was experimentally shown that the effect of electronic absorption in the Pb and Be absorbers before the counter collimator may be calculated by using

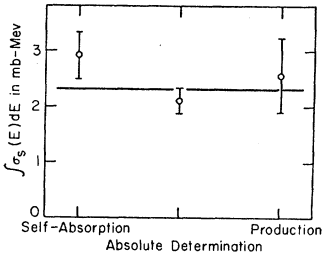

FIG. 14. The value of the integrated scattering cross section, plotted to correspond to the experiment from which it was determined. The horizontal line indicates the weighted mean of the measurements.

narrow beam absorption coefficients (see also reference 5). The correction factor to be applied to $Y(-\frac{1}{2}T)$ for electronic absorption in the lead and the beryllium is 1.257.

The absorption efficiency of the NaI crystal for 15.1-Mev photons, calculated by using the narrow beam absorption coefficients, is 75.6%.

After applying all the above corrections to $Y(-\frac{1}{2}T)$, it is found that $S'=1570\pm168$ where the main contribution to the error is the uncertainty in the extrapolation of the pulse-height spectrum below channel 23 (see Fig. 3).

The target thickness, T, was 2.22×10^{22} C^{12} atoms/cm^2 when the 98.9% natural abundance of C^{12} was taken into account.

Incorporating the above quantities into (12), the value of the scattering integral is found to be $I=2.11\pm0.31$ mb-Mev.

The values of I calculated from the self-absorption, production, and absolute measurements are plotted in Fig. 14. The horizontal line shows the average of the points, weighted according to the reciprocal of the square of the error on each point. The average is 2.33 ±0.19 mb-Mev, and the value of χ^2 for the deviation

of these three points from the average is 2.79, corresponding to a confidence level of about 25%.

PHOTON CASCADES FROM THE GIANT RESONANCE REGION

By lowering the gain of the counter the giant resonance region of the C^{12} can be seen in the same pulse-height spectrum as the 15.1-Mev level. The cross section for scattering of photons of energy roughly corresponding to the energy of the giant resonance may then be estimated relative to the 15.1-Mev peak by assuming all the transitions to be dipole. For 27-Mev bremsstrahlung, the integrated cross section so estimated from this experiment is 0.24 ± 0.05 mb-Mev. The integrated (to 27 Mev) elastic scattering cross section for the C^{12} giant resonance is 0.19 ± 0.05 mb-Mev.[20] The difference, 0.05 ± 0.07 mb-Mev, is assumed to be due to inelastic processes leading to photons in the energy range 18–25 Mev, which corresponds to the interval of summation for the giant resonance in the pulse-height spectrum.

SUMMARY

The angular distribution of scattered radiation from the 15.1-Mev level has been determined to be dipole, over a wide angular range. The magnitude of a nonresonant background to the scattering from the 15.1-Mev level has been determined by fitting the resolution function of the NaI crystal to pulse-height spectra of the 15.1-Mev line, and also by requiring that the self-absorption experiment fit the theoretical attenuation curves for thick absorbers. This background (assumed dipole) as a function of bremsstrahlung energy may be assigned to two causes: (1) scattering from a level near 15 Mev with an integrated scattering cross section 0.10 mb-Mev, and (2) inelastic scattering (leading to 11–18 Mev photons) from levels in the C^{12} giant resonance and having an integrated cross section for this inelastic process of 0.21 mb-Mev.

In the determination of the parameters of the 15.1-Mev level in C^{12}, three distinct experiments were performed. The self-absorption experiment determined the value of the peak cross section and of the ratio of Doppler broadening to level total width. The production experiment gave another determination of that ratio. The absolute cross section measurement determined the value of the integrated elastic scattering cross section for this level.

A summary of the parameters determined for the level is given in Table I with a column indicating the results of the National Bureau of Standards experiment.[5] The second entry is an average of values of δ/Γ determined in the self-absorption and production experiments. The level total width is derived from the second entry by assuming a value of 40 ev for the Doppler width for the scatterers and absorbers employed in the experiment. The radiation width to the ground state of C^{12} is determined from the first and third entries in the table in the manner described at the end of the self-absorption experiment section. The radiation width to the first excited state of C^{12} is found by applying the branching ratio for this transition (obtained from fitting the counter resolution function to the pulse-height spectrum for the scattering with the nonresonant background subtracted) to the fourth entry in the table. The alpha-particle width to the 2.9-Mev (1+) state of Be^8 (decay to the 0+ ground state is forbidden by conservation of angular momentum and parity) is determined as the difference between the total level width and the radiation widths to the ground and first excited states. This is to be regarded as an upper limit since radiative transitions to higher excited states in C^{12} would not be detected in this experiment. It is noted that entries 3-6 (all the width estimates) are derived more or less directly from the assumed value of $\delta=40$ ev, and are directly proportional to this value. The values of the integrated scattering cross section calculated from the parameters of the self-absorption and production experiments are also proportional to δ and those values, averaged with the absolute determination, constitute entry 7 in the table. On the basis of a χ^2 test, the average value in entry 7 has a confidence level of about 25%.

A value of 0.05 ± 0.07 mb-Mev for the integrated (to 27 Mev) inelastic scattering cross section for producing 18–25 Mev photons has been determined. This compares to the elastic scattering cross section (integrated to 27 Mev) for the C^{12} giant resonance region of 0.19 ± 0.05 mb-Mev.[20]

Wilkinson has tabulated[21] values of the transition strength $|M|^2$, the ratio of level radiative width to the quantity $0.021E_\gamma^3$ (the well-known Weisskopf estimate on an independent-particle model for the $M1$ radiative width). Wilkinson finds a flat distribution of values for $|M|^2$, ranging from about 0.005 to 5.0, with 15% of the 40 tabulated values greater than 0.84. The value of $|M|^2$ obtained for the 15.1-Mev transition from the results of this experiment is 0.84, indicating that this is not an unusually strong transition.

Kurath[22] has calculated the transition strength Λ for the $M1$ transitions from the 15.1-Mev level to the ground and first excited states of C^{12} on the basis of an intermediate coupling shell model. Λ is presented as a function of a parameter a/K, which measures the relative strength of spin-orbit and central energies introduced in the model. He defines $\Lambda\equiv\Gamma_\gamma/(2.76\times10^{-3}E^3)$, so for the ground state transition, this experiment

[20] From a slide presented by E. Fuller at the 1957 Photonuclear Conference in Chicago (unpublished).

[21] D. H. Wilkinson, Phil. Mag. **1**, 127 (1956).

[22] D. Kurath, Phys. Rev. **106**, 975 (1957).

implies $\Lambda(\text{G.S.})=6.2\pm1.0$, and for the transition to the 4.43-Mev first excited state, $\Lambda(4.43)=0.9\pm0.7$. From Table I in Kurath's article, one has $\Lambda(\text{G.S.})=5.74$, $\Lambda(4.43)=0.66$, for $a/K=6.0$. The transition to the first excited state is calculated to be more than 95% $M1$ for $a/K>4$. The theoretical and experimental results agree when a/K lies between about 5.5 and 6.7, which Kurath states is a reasonable value for nuclei of mass number 12.

ACKNOWLEDGMENTS

The author wishes to thank Dr. Alan Penfold for his many contributions to this work, and for many helpful discussions concerning it. Thanks is also rendered to the betatron section at the National Bureau of Standards for the calibration of the Kerst-Edwards ionization chamber, and to Dr. Evans Hayward and Dr. Everett Fuller for the calculation of the theoretical curves of Fig. 9.

PHYSICAL REVIEW VOLUME 114, NUMBER 1 APRIL 1, 1959

Excitation Functions of Bismuth and Lead*

W. J. Ramler, J. Wing, D. J. Henderson, and J. R. Huizenga
Argonne National Laboratory, Lemont, Illinois

(Received November 14, 1958)

Cross sections for the reactions $Bi^{209}(He^4,2n)At^{211}$, $Bi^{209}(He^4,3n)At^{210}$, and $Bi^{209}(He^4,4n)At^{209}$ were measured with helium ions of energies from 20.6 to 43.3 Mev. Cross sections for the reactions $Bi^{209}(d,p)$RaE, $Bi^{209}(d,n)Po^{210}$, $Bi^{209}(d,2n)Po^{209}$, $Bi^{209}(d,3n)Po^{208}$, and $Pb^{208}(d,p)Pb^{209}$ were measured with deuterons of energies from 6.3 to 21.5 Mev. Some information is presented on the $Bi^{209}(He^4,t)Po^{210}$ reaction. A half-life of 7.23 ± 0.04 hr was measured for At^{211}. The $Bi^{209}(d,3n)Po^{208}$ threshold energy is 12.0 ± 0.3 Mev (center-of-mass system). The compound nucleus reaction cross sections are compared with the predictions of the Jackson model, and good agreement is obtained. The (d,n) and (d,p) stripping cross sections are discussed briefly.

INTRODUCTION

THE direct comparison of nuclear reactions of fissionable with nonfissionable materials allows one to draw certain conclusions about the mechanisms of these reactions. The elements lead and bismuth have extremely small fission cross sections[1] at the charged-particle bombarding energies used in this study, whereas isotopes of thorium, uranium, and other heavy elements have relatively large fission cross sections.

Bismuth is a convenient target for excitation function work with light projectiles since the resulting polonium and astatine isotopes are alpha emitters. In an earlier paper we reported results obtained from the bombardment of bismuth with 10.65-Mev protons.[2] Other investigators have bombarded bismuth with 19-Mev deuterons and 38-Mev helium ions.[3] However, it seemed worthwhile to extend the $(d,3n)$ and $(He^4,3n)$ measurements to slightly higher energies and to study the $(He^4,4n)$ reaction cross sections as a function of helium-ion energy. In addition, the $(d,2n)$ excitation function was established more accurately by examining the alpha activities of the target samples three years after the completion of bombardment. Since Po^{209}, the product of the $Bi^{209}(d,2n)$ reaction, has a long half-life compared with Po^{210}, a quantitative assay of Po^{209} by alpha-particle energy analysis is possible for some bombarding energies only after the gross polonium alpha activity has decayed by many factors.

The (d,p) excitation function obtained for bismuth represents only the reaction leading to the 5.0-day RaE isomer of Bi^{210}. The 2.6×10^6-yr isomer of Bi^{210} has too long a half-life for detection in the present experiments.

A study of the reaction $Pb^{208}(d,p)Pb^{209}$ was made in order to compare its excitation function with (1) the (d,p) excitation function of a fissionable material and (2) the excitation function obtained for the $Bi^{209}(d,p)$RaE reaction in search for indirect evidence that part of the bismuth reaction resulted in the long-lived isomer of Bi^{210}.

EXPERIMENTAL PROCEDURE

The bismuth plates were prepared by the technique previously described.[2] Bismuth metal was evaporated onto aluminum disks of 0.0005-inch thickness. The amount of bismuth on each target varied from 50 to 100 $\mu g/cm^2$. The weight of bismuth was determined, after the necessary counting data had been taken, by a colorimetric procedure.[2] The lead samples were lead foils of about 11 mg/cm^2 thickness.

The stacked-foil technique was used to obtain the desired energies of the bombarding particles. Blank aluminum foils of known weight were inserted between the

* Based on work performed under the auspices of the U. S. Atomic Energy Commission.

[1] A. W. Fairhall, Phys. Rev. **102**, 1335 (1956); E. F. Neuzil and A. W. Fairhall (private communication).

[2] Andre, Huizenga, Mech, Ramler, Rauh, and Rocklin, Phys. Rev. **101**, 645 (1956).

[3] E. L. Kelly and E. Segrè, Phys. Rev. **75**, 999 (1949).